Kinematic Analysis of Human Movement: Gait and Mountain Climber

Ana Lopes (98587)[1], Daniel Galhoz (90791)[2], Mariana Mourão (98473)[3] and Rita Almeida (90180)[4]

[1] *Instituto Superior Técnico,*
Integrated Master's in Biomedical Engineering,
ana.rita.santos.lopes@tecnico.ulisboa.pt

[2] *Instituto Superior Técnico,*
Integrated Master's in Biomedical Engineering,
daniel.galhoz@tecnico.ulisboa.pt

[3] *Instituto Superior Técnico,*
Integrated Master's in Biomedical Engineering,
mariana.mourao@tecnico.ulisboa.pt

[4] *Instituto Superior Técnico,*
Integrated Master's in Biomedical Engineering,
rita.margarida.almeida@tecnico.ulisboa.pt

ABSTRACT — *The kinematic analysis of human motion is extremely important in several areas. In medicine it can be used for therapeutic and diagnostic, whereas in sports to evaluate performance and detection of injuries. Therefore, the goal of this paper was to describe and study, through a kinematic analysis, two movements in the sagittal plane – the gait cycle and the mountain climber exercise in a multibody biomechanical system. The data was acquired in the Biomechanics of Motion Laboratory at Instituto Superior Técnico and the 2D Multibody Model was defined with MATLAB. Regarding the gait cycle, the velocity and the movement of the subject, the angle of the hip, knee and ankle and the* displacements *and velocity of the right foot were analyzed. Comparing with the literature, the discrepancies found in the cadence and velocity, being lower than expected, and angles obtained, higher than expected, can be explained through the conditioning of the subject in stepping on the targets placed on the floor. This caused the delivering of a slower gait motion and the lifting of the lower limbs at higher altitudes to reach the pre-defined positions. As for the mountain climber, the angles of both knees and hip were analyzed as well as the posture of the subject and found that, although there was no viable information or literature to support this, the movement did not have the best performance in terms of knee flexion. It was intended to start the flexion of the opposite knee while the other is extending, and this was not observed. Nevertheless, the mathematical model implemented demonstrated good and coherent results that allowed a detailed analysis of the movements.*

1 Introduction

Kinematics concerns the study of the spatial movement of the body, independent of the forces that caused the said movement, dealing with measurements of kinematic variables: displacements, joint angles, velocities and accelerations.[1] Regarding a multi-body system, the kinematic analysis involves the assessment of these kinematic variables for each body segment, by formulating and solving the equations of motion.

These basic kinematic concepts are taught in a two-dimensional system, where the anatomical segments correspond to rigid bodies and the articulations are represented by geometrically ideal or contact mechanical joints. This implementation is viable if the movement under analysis is mainly performed in a plane.[2] Considering this, the motions chosen to study in this paper occur predominately in the sagittal plane: the gait, already highly analyzed in literature, and the mountain climber exercise.

1.1 Description of the motion

1.1.1 Gait

The gait movement is the most common of all human actions. This motion is a repetition of gait cycles, with each cycle involving a step of one foot followed by a step with the opposite foot. Each step corresponds to the events occurring between the heel strike of one leg and of the contra-lateral leg, with two steps being the stride parameter referred as one complete gait cycle. The arms help to maintain a good balance, adding some momentum when accompanying the movement of the legs during the stride. In Figure 1.1 is shown one complete gait cycle.

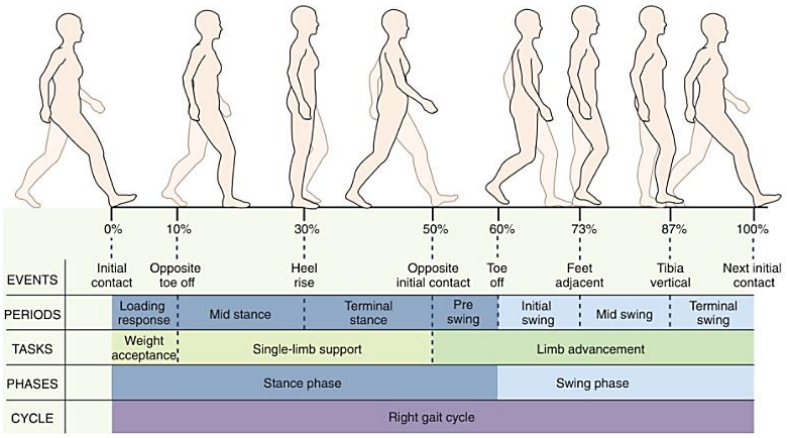

Figure 1.1: Gait cycle. [3]

When describing the gait cycle, there is specific terminology, certain events, and important phases to be considered. Composing the initial 60% of the gait cycle, there is the **stance phase**, which for one reference foot regards its support, weightbearing and overall stability roles, being always in contact with the ground. It begins with an *initial contact* of the considered foot, or shoe, with the ground, initializing the *loading response* of the gait cycle, which ends the moment the contra-lateral foot leaves the ground. The next stage, *mid-stance*, extends to when the center of mass is vertically aligned with the reference foot. This gives rise to the *terminal stance* stage, ending at the instant of the contra-lateral leg heel strike. This phase ends when the toe of the foot leaves the ground (*toe off*), consisting in the *pre-swing* stage. The following phase is referred as the **swing phase,** which composes the other 40%. In this phase, the reference foot is in the air, being accelerated forward to the *mid-swing* (when the tibia of the swing limb is vertical) and decelerated towards the next contact with the ground. As the foot makes contact again with the ground, the stride ends, and a new gait cycle begins.[3] [4]

The parameters frequently assessed to characterize gait are simple temporal and length measurements, such as *step length* – the distance between the heel contact point of one foot and that of the other foot –, s*tride length* – the distance between the successive heel contact points of one foot – and *cadence* – the walking rate expressed in steps per minute (step/min). [5] These parameters are illustrated in Figure 1.2.

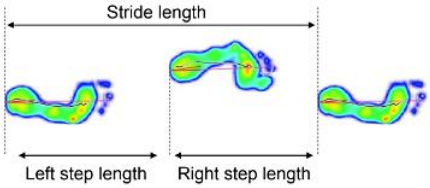

Figure 1.2: Gait parameters.[5]

1.1.2 Mountain Climber

The mountain climber, also known as running plank, is a dynamic and compound exercise, consisting of being in a plank position and bringing the knees into the chest, while alternating the legs. By involving constant, smooth and repetitive movement, the motions performed throughout the exercise engage with several different joints and muscle groups, managing to do a total-body workout with just one exercise, having as purpose the building of core strength, endurance and stability, as well as agility. When performed at a rapid pace, it is also an effective form of cardiovascular training. [6] [7][8]

This exercise starts from a high plank position, where the arms are flexed, the hands are shoulder-width apart, with a slight ulnar deviation, and the legs are extended behind, with the weight being distributed between the hands and the dorsiflexed feet. Then, by doing a flexion of both the upper and lower leg, the knee is pulled toward the chest, while trying to keep the hips aligned with the trunk. After that, the leg is extended and brought back to its initial position in the plank to repeat the previous motion with the opposite leg.

Figure 1.3: Mountain climber exercise. [9]

Given that each repetition of the exercise involves flexion and extension of the hips and knees, the range of angular amplitudes of these joints is overall improved, thus boosting athletic performance and lowering the susceptibility to injury.[6] As for the endurance, strengthen and stability of the core muscles, it ensures spine stability, allowing a proper alignment for posture and gait. Performing the mountain climber movement can evaluate resistance, mobility, and coordination, as well as overall health.[10]

2 Methodology

2.1 Experimental Data Acquisition

Intending to biomechanically study the dynamic movements proposed, it was performed a laboratory session organized at Instituto Superior Técnico's Biomechanics of Motion Lab. There, 19 passive light-reflecting markers were placed on specific anatomical landmarks of a volunteer, representative of joints and bone extremities. The motion capture system (MOCAP), composed of 14 IR optical cameras (QualisysProReflex 500/1000), allowed the spatial tracing of the volunteer's movement. [11]

The desired output of the data collection stage for the kinematic analysis is a file of the x, y, z coordinates for each of the markers at each sample point in time (digitalized data), saved in three data files (one for each movement). These coordinates are in the global reference system (GRS) that is fixed in the laboratory.

Additionally, electromyography data, ground reaction force and the center of pressure were collected, with the former being recorded by four electrodes placed on leg muscles (Gastrocnemius Medialis, Tibialis Anterior, Rectus Femoris and Biceps Femoris), and the last two by 3 force plates positioned on the floor, which the volunteer had to walk in. Regarding the kinematic analysis to be performed, this data was not analyzed.

2.2 Formulation of the Multibody Model System

The analysis of the multibody system was performed in the 2D sagittal plane, implying the projection of the 3D raw data onto the former, that is, only considering the x and z coordinates. Of the 19 markers, both side heel points were not considered. Moreover, resulting from the projection, for the body segments which had two markers (hips and shoulders), it was computed their midpoints. Taken into consideration the aforementioned, it was obtained a model with 15 points, being each body characterized by two points (proximal and distal points), thus obtaining 14 bodies, considering 13 revolute joints in the model formulated (Figure 2.1).

For a 2D model, each body *i* has a vector of coordinates q_i given by its center of mass (CoM) position r_i and orientation θ_i of the body-fixed coordinate system $\xi_i\eta_i$, both relative to the GRS. This angle is considered positive if the rotation from positive x axis to positive ξ_i axis is counterclockwise.

$$q_i = \begin{bmatrix} r_i \\ \theta_i \end{bmatrix}, r_i = \begin{bmatrix} x_i \\ z_i \end{bmatrix} \quad (1)$$

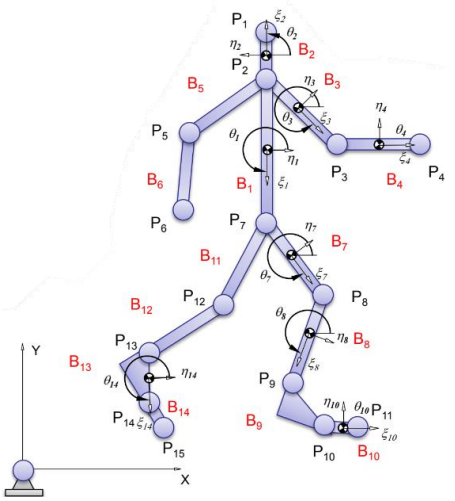

Figure 2.1: Schematic representation of the 2D biomechanical model considered, having 14 bodies (B_1 to B_{14}) and 15 points representing markers (P_1 to P_{15}). [5]

In order to perform the kinematic analysis, the number of constraint equations must equal the number of coordinates. Since there is a total of 42 coordinates (3 per body), and the 13 revolute joints only introduces two kinematic constraints (constraining 2 degrees of freedom - 2 translations - in 2D, only allowing one rotation between the two connected rigid bodies), it remains 16 constraint equations, which describe the motion of the system's 16 driving degrees of freedom. For this model, it was considered two types of drivers:

- Drivers of type I (3 implemented) nominated simple drivers, which considers a uniform accelerated system, describing altogether the position and orientation of the whole system.
- Drivers of type III (13 implemented), each describing the angle between two vectors of two different bodies connected by each of the 13 revolute joints.

The model described was written in text format (DraftBiomechanicalModel.txt), being in terms of anthropometric variables: location of the CoM of each body as a percentage of the segment length from either their distal and proximal points; local coordinates of the revolute joint with respect to the CoM of the connected bodies, normalized by the length of the segment. The file follows a structure, which is specified in Appendix A.

2.3 Pre-processing

The pre-processing stage consists in organizing the raw data files, relative to the two dynamic movements, into files for the kinematic analysis code.

Firstly, it is applied the function *ReadProcessData.m*, which receives one of the tsv raw data files and stores the x and z coordinates of each marker for each time frame. Then, due to noise content mainly introduced by the human digitizing process [1], a fourth-order zero-lag Butterworth low-pass digital filter was applied by the function *FilterCoordinates.m*, using the MATLAB built-in functions *butter.m* and *filtfilt.m*. The selection of the cut-off frequency, f_c, was achieved through a residual analysis of the difference between the filtered $\hat{X}_i$ and unfiltered X_i signals, computed over a determined range of cut-off frequencies (0.1 Hz to 15% of the sampling frequency, for a step of 0.1 Hz). For each f_c, the residual $R(f_c)$ is expressed as follows:

$$R(f_c) = \sqrt{\frac{1}{N}\sum_{i=1}^{N}\left(X_i - \hat{X}_i\right)^2} \tag{2}$$

being N the number of samples in the signal analyzed. For the residual plots obtained for each marker and each coordinate, a linear regression was performed, considering as the stopping criteria the correlation for the linear regression R^2 (minimal value of 0.92). Upon defining the best linear fit, it is computed the ordinate-intercept (at 0 Hz), which is approximately equal to the Root Mean Square (RMS) value of the noise, since the $\hat{X}_i$ for a 0-Hz filter is the mean of the noise over the N samples [1]. The cut-off frequency is then defined as the frequency in the residual plot for which that residual is obtained. In the Appendix B, it is displayed the residual plot and the corresponding comparation between the filtered and non-filtered gait data for the z-coordinate of right knee body.

After filtering, the coordinate data is organized into a data structure, according to the definition of the biomechanical model (x and z coordinates for points P1 to P15). Since the input data file that describes the 2D multibody system (read and stored by the function *ReadDraftInput.m*) is in terms of anthropometric variables, the initial phase of the pre-processing stage concerns the computation of the body segments' length (*ComputeAverageLength.m*), by analyzing a static position in which the subject is in the anatomical reference position. Due to the projection of the coordinate data, inconsistencies in the length of bodies segment in each time frame arise. Therefore, an average length is computed for each body considering all the frames, being the length in each time frame computed as the distance between the proximal P_i and distal P_j points of the body.

Regarding the positions and angles for all the bodies, the function *EvaluatePositions.m* applies the following reasoning:

$$r_i = r^{P_i} + A_i s_i'^{P_i} \tag{3}$$

$$\theta_i = cos^{-1}(\xi_i)\ , \tag{4}$$

with r_i being the CoM position of the body i relative to the GRS, r^{P_i} the position of the proximal point P_i relative to the GRS, A_i the rotation matrix and $s_i'^{P_i}$ the position of point P_i in the local reference frame of the body. Note that, since the anthropometry data considers that the CoM is aligned with the proximal and distal point, the η_i component is 0, being $s_i'^{P_i}$ the ξ_i position of CoM with respect to P_i (unnormalized anthropometry data).

As for the drivers, the function *EvaluateDrivers.m* computes the variation of the driving degrees of freedom of the multi-body system, that is, the variation of the system position and angle with time for drivers of type I, and variation of joint angles θ_{ij} with time for drivers of type III :

$$\theta_{ij} = \theta_j - \theta_i\ , \tag{5}$$

with θ_j and θ_i being the orientation of the local reference frame of the connected bodies in relation to the GRS, being defined with respect to the horizontal x-axis and measured counterclockwise.

Finally, the function *WritesModelInput.m* organizes the data regarding the model's initial configuration, saving into a file named "BiomechanicalModel (motion name, either gait or mountain_climber).txt". Additionally, it creates text files with the updated driver's temporal data, named "(motion name, either gait or mountain_climber)(number of driver, 1 to 16).txt". The structure of the output file is displayed in Appendix C.

2.4 Processing

Given the initial configuration of the system and its driving degrees of freedom over time, the kinematic analysis consisted in determining the position, velocity and acceleration of all bodies, at any given instant t, by solving the constraint equations (imposed by the revolute joints and the drivers) and its two first order time derivatives for that instant. In Table 2.1 are presented the constraint equations.

Table 2.1: Constraint equations for revolute joints and drivers of type I and III.

	Constraint Equations	**Number Implemented**
Revolute Joints	$\Phi^{(rev,2)} = (r_i + A_i s_i'^P) - (r_j + A_j s_j'^P) = 0$	13
Drivers of Type I	$\Phi^{(drv1,1)} = z_i - z_i(t) = 0$, with z_i being either z_i, x_i or θ_i	3
Drivers of Type III	$\Phi^{(drv3,1)} = \theta_{ij} - \theta_{ij}(t) = 0$, with $\theta_{ij} = \theta_j - \theta_i$	13

Initially, it is necessary to perform an interpolation of the position, velocity, and acceleration for each driver as a continuous function of time (function *ReadInput.m*). From the MATLAB built-in function *spline.m*, it was performed a cubic interpolation of the position, returning the coefficients of the interpolated polynomial. For the first and second-order derivatives of the interpolated function, it was used the MATLAB built-in function *polyder.m*. Similar to what was performed in the pre-processing stage for the spatial coordinates, the first and second-order derivatives were filtered (function *FilterCoordinates.m*). Note that the applied residual method can deliver nonoptimal cut-off frequencies for higher-order derivatives. An alternative method is described by Yu et al. (1999), having obtained higher cut-off frequencies than those estimated for the displacement residual analysis[1].

The implementation of the position, velocity and acceleration analysis was done by the functions *PositionAnalysis.m*, *VelocityAnalysis.m* and *AccelerationAnalysis.m*, mathematically described as follows:

$$\begin{cases} \Phi(\mathrm{q},\mathrm{t}) = 0 \\ \dot{\Phi}(\mathrm{q},\mathrm{t}) = 0 \\ \ddot{\Phi}(\mathrm{q},\dot{\mathrm{q}},\mathrm{t}) = 0 \end{cases} \text{ with } \begin{cases} \dot{\Phi}(q,t) \Leftrightarrow \Phi_q \dot{q} = \nu \\ \ddot{\Phi}(\mathrm{q},\dot{\mathrm{q}},\mathrm{t}) \Leftrightarrow \Phi_q \ddot{q} = \gamma \end{cases}, \tag{6}$$

being the jacobian matrices Φ_q, $\dot{\Phi}_q$ and $\ddot{\Phi}_q$ computed with the function *FuncEval.m*, which has as auxiliary functions the *JntRevolute.m* and *JntDriver.m*, respectively computing the constraint equations given by the revolute joints and the drivers.

Since the constraint equations for the revolute joints are non-linear, the position analysis consists of a system of non-linear equations, being its resolution implemented by the Newton-Raphson method, which is typically used for having a quadratic convergence, that is, the error at each iteration is proportional to the squared error at the previous iteration [12]:

$$\begin{cases} q_{i+1} = q_i - [\Phi_{q_i}(q_i,t)]^{-1}\Phi(q_i,\mathrm{t}) \\ |q_i - q_{i+1}| = |\Delta q_i| \leq \varepsilon \end{cases}, \tag{7}$$

with ε being the threshold for the maximal magnitude residual of the vector $|\Delta q_i|$, having been stablished to 10^{-6}. Note that the initial estimate q_0 regards the initial positions of the system, given as input to the kinematic analysis code. Additionally, it was imposed a limit of 12 iterations for the iterative process, to prevent the entrance on an infinite loop. Regarding the velocity and acceleration analysis, it is obtained linear equations for the generalized velocities and acceleration of the system, being analytically solved.

3 Results and Discussion

In this section, it is presented the results obtained through the computational implementation of the kinematic analysis regarding the performance of both our movements – gait and mountain climber. Whenever possible, the results obtained are compared with the ones from the literature, as a form to assess the subject's structural and functional integrity of its biomechanical system, as well as to validate our computational implementation.

3.1 Gait movement

As was aforementioned in the introduction of the gait movement (1.1.1 section), one complete gait cycle concerns two phases: firstly, the Stance Phase, which corresponds to approximately 60% (58-61%) of the entire cycle, whereas the second phase, called Swing phase, correlates to the others 40% (39-42%).[4] [8] From the data collected, it was obtained a stance and swing phases of 58.5% and 41.4%, respectively, being inside the percentage range expressed in the literature for both phases.

Regarding a pictorial and anatomical description of the dynamics in the plane of the gait movement, a stick diagram can be obtained (Figure 3.1) by plotting, at equal intervals of time, each body segment as a straight line or stick [1] [13]. From the stick diagram, as well as from the temporal information regarding one complete gait cycle, it can be extrapolated the following gait parameters previously introduced (1.1.1 Section): cadence (step/min), by considering 2 steps for a gait cycle with a duration of 1.43 s, resulting in a cadence of 89.55 step/min; stride length (m), which can be derived from the initial and final position of the toes in the one complete gait cycle, obtaining the value of 1.18 m; velocity (m/s), computed as:

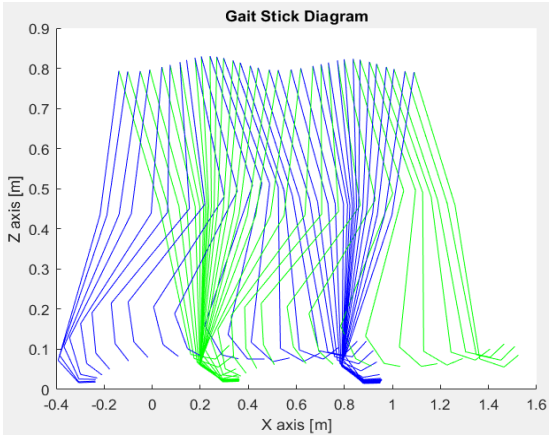

Figure 3.1: Display of the animation regarding the sagittal plane (X and Z) positions of the lower body. The green lines represent the right lower body whereas the blue ones to the left lower body.

$$v = \frac{stride \times cadence}{120}, \quad (8)$$

obtaining a value of 0.89 m/s. On the Biomechanical Laboratory, for a total of 41 steps, the mentioned parameters show discrepancies with the ones previously extrapolated just from one complete gait cycle (2 steps). This can be explained by the inherent and inevitable intra-subject variability, being more statistically significant the parameters assessed for a larger sample size. In that sense, taking into consideration the volunteer characteristics (age and sex), in table 3.1 is displayed the expected parameter values alongside the experimentally 41 steps.

Table 3.1: Comparison between the literature and the data acquired from the laboratory results for one full cycle.

	Stance phase [%]	**Swing Phase [%]**	**Cadence [steps/min]**	**Cycle time [s]**	**Stride length [m]**	**Velocity [m/s]**
Data collected in the Lab	58.5	41.4	115.3	1.04	1.19	1.14
Data form literature [14] - female, ages between 20-29	-	-	124.8	-	1.18	1.24
Data form literature [4] - female, ages between 18-49	58-61	39-42	98-138	0.87-1.22	1.06-1.58	0.94-1.66

For the study that considers woman with ages between 20-29, both the velocity and the cadence are lower than their references, being the stride length the closest. This suggests that the performed gait motion was slower than normal gait, which can be explained by the simultaneous acquisition of kinematic and dynamic data, being the subject's gait conditioned to the 3 force plates positioned on the floor, which the volunteer had to walk in, possibly

leading to higher length and time duration steps. Although the subset of women in this first study is more representative of our subject´s age, the same parameters assessed in the second study (subset of women with age 19-49), contain the values experimentally obtained. This draws the attention regarding the conclusions derived from comparison with reference data, since both inter- and intra-subject variability impairs the interpretation.

For a more complete assessment of the volunteer's gait movement, an evaluation of all the rigid bodies and respective joints would be more suited, as it affects them all and would be useful to study possible pathologies. However, it is important to recall that, by definition, joint angles are relative and, therefore, do not give information about the absolute angle of each of the adjacent segments in space. Since in normal walking the trunk can be considered to be almost vertical (actually it is biased slightly forward of vertical), the hip angle constitutes a good estimate for the thigh's orientation in space, whereas the knee angle would yield the leg angle and the ankle angle would give a reasonable estimate of foot angle in space. [13] For this reason, it will be presented graphical comparisons with the literature regarding the hip, knee, and ankle joints angles, as well as plots of the velocities and displacements for the metatarsal.

3.1.1 Lower Limb Angles Displacements

For the joint angle displacements over one complete gait cycle, it was obtained an approximate match of the shapes of the curve with the ones from the literature, supporting the hypothesis of a correct kinematic analysis implementation. However, in order to standardize the obtained angle displacements with respect to the literature, it was added a personalized constant to the joint angles of the knee and ankle.

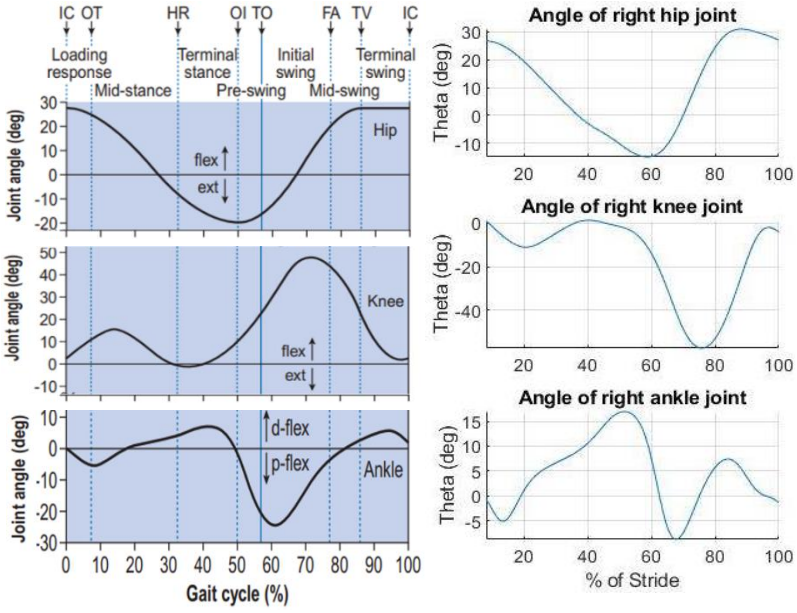

Figure 3.2: Sagittal plane of right hip, knee, and ankle joint angles. (Left) Retrieved from Whittle.[4] (Right) Results acquired with the MATLAB implementation.

Regarding a more in-depth analysis of the angle displacements, for the hip joint, which connects the trunk and tight, the profile of the curve follows the predicted shape: initial extension of the hip until the pre-swing phase of the gait cycle, where it reaches hyperextension, being subsequently followed by hip flexion. At the end of one full gait cycle, it was supposed to reach an approximately stationary value, although it seems that the analyzed data includes the very initial part of the next gait cycle performed by the subject.

Regarding the knee joint, which connects the tight and leg, it is obtained an inverted curve in relation to its reference, being explained by opposite senses involved in their measurements. Taking this into account, once again the range of angular amplitude is slightly bigger (in the swing phase, the knee flexion reaches a maximal

value of 60º, whereas in the reference graph is below 50º), giving additional evidence that the subject wasn't performing a normal gait motion, forward-leaning the leg in a higher angular amplitude to delivering longer steps for walking over the force plates. However, it was found in the literature similar ranges for normal gait, including for slow cadence gait. [13]

Finally, for the ankle joint, which connects the leg and foot, it is obtained a higher range of angular amplitude regarding the dorsiflexion, and, on the contrary, a lower range for the plantarflexion, both in respect to the literature, once again due to the same reason as mentioned before.

3.1.2 Displacements and Velocities

Regarding the right foot velocities (m/s) in the sagittal plane, as well as its vertical displacement (m), it was performed a side-by-side comparison with references for the right metatarsal, obtained for a sample size of 14 subjects. [13] As can be seen, the velocity and displacement temporal profiles are very similar, supporting the hypothesis that the computational implementation was well succeeded, thus reproducing consistent results for the gait cycle.

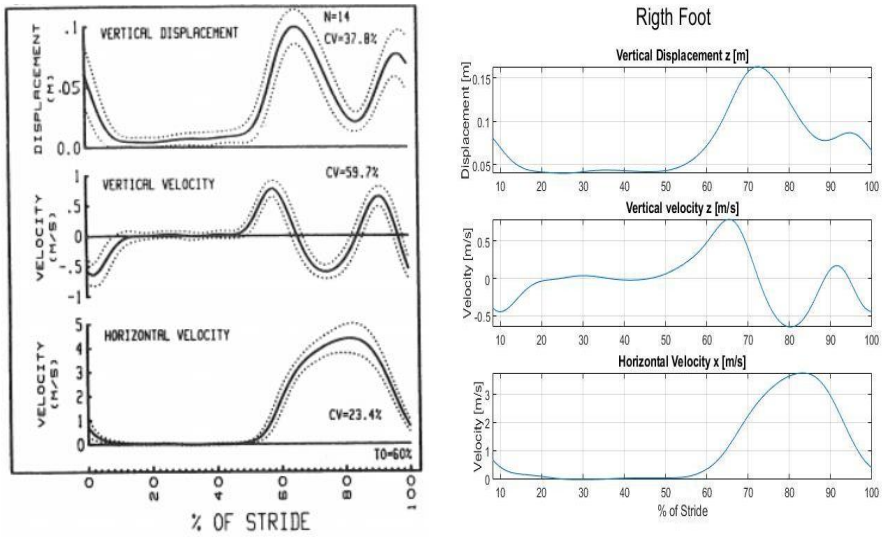

Figure 3.3: Comparison of the vertical and horizontal velocities and the vertical displacement of the metatarsal between the literature and the results obtained with the implementation on MATLAB. (Left) Displacement and velocity of metatarsal.[13] (Right) Displacements and velocity of right foot.

However, certain differences were observed, mainly regarding the vertical displacement and horizontal velocity: the maximal vertical displacement reaches higher values (0.15 m instead of approximately 0.1 m) and, on the contrary, the horizontal velocity is consistently lower over time. Once again, this supports the hypothesis that the subject was delivering a slower gait motion, lifting the lower limbs at higher altitudes in order to reach pre-defined positions (force plates) more distant-apart than a normal stride would require. Nevertheless, it's important to mentioned that the graphics obtained from our kinematic analysis implementation referred to the center of mass of the foot, rather than to a single marker placed in the metatarsal, being another source of impairment in the comparison analysis.

As a final consideration, establishing more standardized protocol acquisitions would be, indeed, advantageous, in order to facilitate cross-validation of results. Moreover, as was evidenced by the comparison with different references in the accessed literature, inter and intra-subject variability play a huge role, being more statistically significant the assessment of larger sample-sized biomechanical motion data. Given this, it can be considered quite remarkable the transversality and precision of the obtained results for just one complete gait cycle, leading to the claim that the gait motion is, indeed, a relevant form of diagnosis.

3.2 Mountain Climber

For the kinematic analysis of the Mountain Climber exercise, it is important to note that it was not possible to compare the obtained results with the literature, since kinematic studies for this movement are scarce.

The obtained data corresponds to various repetitions of this motion, hence it was temporally windowing in order to isolate one-full cycle, in respect to the left knee. Furthermore, the analysis was divided between the lower body and the upper body, with the hip joint discussed in the first.

3.2.1 Lower Body

This movement is composed of 2 major steps, those being the flexion of one knee and hip joint (Figure 3.4 – Left), and the extension of these flexed joints (Figure 3.4 – Right), both alternated on each leg. When we accelerate the pace of this movement, it is necessary to start one step before finishing the other, which will result in lifting the hip, observed in Figure 3.4.

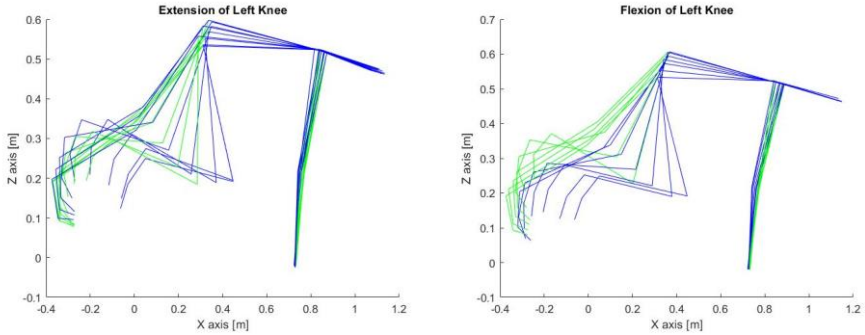

Figure 3.4: Stick diagram of the motion. (Left) Flexion of the left knee and hip. (Right) Extension of the left knee and hip.

The intended way to perform this movement is to start the flexion of the opposite knee while the other is extending, reaching the optimal velocity of the exercise. In this acquisition, this was not observed, as can be seen in Figure 3.5 – Left and Middle –, where the time represents a full cycle regarding the left knee. It was observed that only when the left knee is halfway on extending, the other starts flexing (around the 0.55 second mark), which is not the optimal. This also can be observed in the plateau of the graphs, where the other knee is waiting for the other to end flexing and start extending. Note that, as was concluded for the gait analysis, the angles for the knee joints are inverted.

Regarding the hip joint (Figure 3.5 – Right), it is observed that its movement is synchronized with the knee joint (Figure 3.5 – Middle), and both reach its flexion peak at the same time. With this result, it can be safely concluded that this part of the movement is performed with the maximum efficiency.

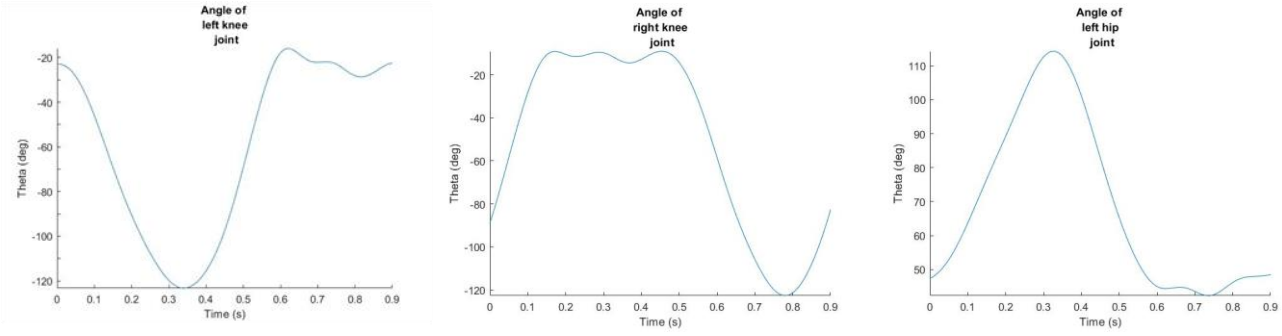

Figure 3.5: (Left) Angle of the left knee joint. (Middle) Angle of the right knee joint. (Right) Angle of the left hip joint.

3.2.2 Upper Body

Because this movement is based on a straight-arm plank, it can be expected the upper body to be in a standstill position, with the head aligned with the spine, and an angle for the shoulder joints of around 90º, which can be confirmed to be true in the stick diagram (Figure 3.4), without any need for further analysis.

For a more in-depth analysis of this exercise, it would have been useful to pair EMG data with the kinematic data, in order to determine muscle contribution during exercise [1] [15], mainly the core muscles (not available in the EMG data provided), which ideally isometrically contract (length of the muscles remains constant) and maintains a neutral alignment of the trunk while performing mountain climbers [6]. Although, as the core muscles fatigue over the execution of this exercise for large periods of time, it may affect the mechanics of the lower extremity joints, as the trunk controls a large portion of the body's center of mass [16]. Moreover, it can lead to back injuries, since in this case the weight of the trunk will be hold by the spine. Therefore, this exercise is not recommended to execute for long periods of time, which will induce fatigue and provoke poor form, or muscle failure. [17]

4 Conclusion

Intending to assess the locomotive human system, namely the kinematic motion of a supposedly healthy subject, a computational implementation was developed for a kinematic analysis, considering a 2D multibody system. From the applied methodology, kinematic variables (positions, velocities, accelerations, and angles) for body joints and segments were evaluated over time.

Regarding the gait cycle, the results obtained are mostly in accordance with the revised literature, validating the constructed 2D model as an approximation for the locomotion, as well as the computational implementation developed. The deviations observed, mainly supporting the hypothesis that the subject was delivering a slow gait rather than normal gait, were attributed to the non-ideal experimental conditions: the subject's gait was conditioned to the 3 force plates positioned on the floor; skin movement artifacts, that is, displacement of the markers from their anatomical landmarks due to the skin sliding over the bones. The computational methods applied could also explain the observed differences, such as the filtering process and the multibody model chosen, being the accuracy of the analysis dependent as much on the quality and completeness of the anthropometric measures as on the kinematics data. Furthermore, inter- and intra-subject variability must be taken into account when cross-validating results with the literature, being more statistically significant the assessment of larger sample-sized biomechanical motion data.

As for the mountain climber movement, the comparison with references was not possible, due to the lack of kinematic studies regarding this motion. Nevertheless, even though the acquisition analyzed was enough to understand the kinematics of the system, its overall performance was poor, since the movement could be optimized.

References

[1] David A. Winter, Biomechanics and Motor Control of Human Movement. Hoboken, New Jersey: John Wiley & Sons, Inc., 4 ed, 2009.

[2] H. Oliveira, "Inverse Dynamic Analysis of the Human Locomotion Apparatus for Gait", MSc Thesis in Biomedical Engineering, Instituto Superior Técnico, Universidade de Lisboa, 2016.

[3] Donald A. Neumann, Kinesiology of the Musculoskeletal System: Foundations for Rehabilitation, pp. 631-637. Missouri: Mosby Inc., 2 ed, 2010.

[4] Michael W. Whittle, Gait Analysis: An Introduction, pp. 52-59 and 223. Oxford: Butterworth-Heinemann Ltd., 4 ed, 2007.

[5] IST Integrated Master's in Biomedical Engineering, "Biomechanics of Human Motion 2020-2021 - week 07 (Practical)", 2020.

[6] "MOUNTAIN CLIMBERS", available at https://www.wilsonpt.com/dt_workouts/mountain-climbers/. Accessed in 24-11-2020.

[7] "What Are the Benefits of Mountain Climber Exercise?", available at https://livehealthy.chron.com/benefits-mountain-climber-exercise-2077.html. Accessed in 25-11-2020.

[8] "PHYSICAL CONDITIONING FOR MOUNTAINEERS", available at https://firstlightguiding.com/mountaineering-fitness/. Accessed in 22-11-2020.

[9] "Mountain Climbers Steps Sequence Health Fitness Exercise PE Secondary Bw RGB", available at https://www.twinkl.it/illustration/mountain-climbers-steps-sequence-health-fitness-exercise-pe-secondary-bw-rgb. Accessed in 24-11-2020.

[10] Hollis Lance Liebman, Core Fitness. New York: The Rosen Publishing Group, Inc., 1 ed, pp 13 and 56-57, 2015.

[11] IST Integrated Master's in Biomedical Engineering, "Biomechanics of motion laboratory guide," first semester 2020/21.

[12] IST Integrated Master's in Biomedical Engineering, "Biomechanics of Human Motion 2020-2021 - week 02", 2020

[13] David A. Winter, The Biomechanics and Motor Control of Human Gait. Waterloo, Ontario, Canada: University of Waterloo Press, 2 ed, 1988.

[14] R. B. Dale, "21 - clinical gait assessment," in Physical Rehabilitation of the Injured Athlete (Fourth Edition) (J. R. Andrews, G. L. Harrelson, and K. E. Wilk, eds.), pp. 464 – 479, Philadelphia: W.B. Saunders, fourth edition ed.,2012.

[15] "Plank and Side Plank Progressions", available at https://brookbushinstitute.com/article/plank-progression?fbclid=IwAR21dRz-LKk9gCZZDHlwMc7HYDSnMn_r8U3HofRq-VwAtep9czD3n5yofLk. Accessed in 20-11-2020.

[16] Hung K-C, Chung H-W, Yu CC-W, Lai HC, Sun F-H (2019) Effects of 8-week core training on core endurance and running economy. PLoS ONE 14(3): e0213158. https://doi.org/10.1371/journal.pone.0213158.

[17] "Building ab strength for every female client", available at https://www.fitnessnetwork.com.au/resources-library/building-ab-strength-for-every-female-client/. Accessed in 27-11-2020.

Appendix A

Table A.1: Structure considered for the input file of the 2D biomechanical multibody, DraftBiomechanicalModel.txt, read by the function *ReadDraftInput*. Values for the position of the PCoM, ζ/L and η/L were accessed from [5].

NBodies	**NRevolute**		**NGround**		**NDriver**	
Body number (1, ..., 14)	Proximal Point, P_i		Distal Point, P_j		PCoM	
Joint Revolute number (1, ..., 13)	Proximal Body, i	Distal Body, j	ξ_i/L_i	η_i/L_i	ξ_i/L_j	η_i/L_j
Joint Driver number (1, ..., 16)	Type	Proximal Body	Coordi	Distal Body	Coordj	Filename
	I	i	1, 2, 3	-	-	.txt
	III	i	-	j	-	.txt

Appendix B

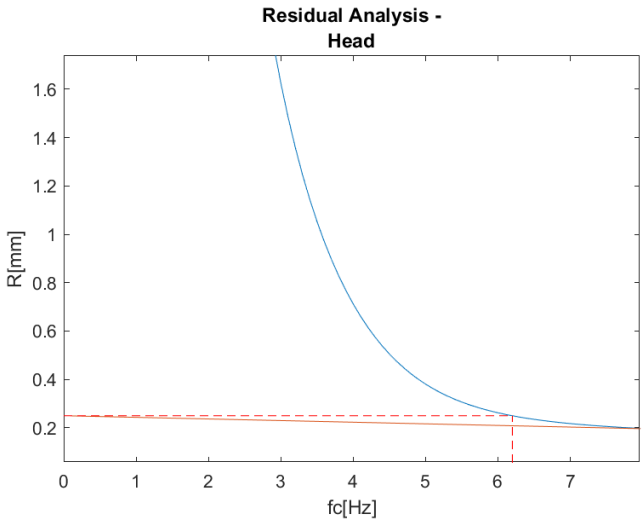

Figure B.1: Residual analysis for the Z-coordinate of the head, considering a range of frequencies of 0.1Hz to 15% of the sampling frequency, for a step of 0.1 Hz. The obtained cut-off frequency was 6.2 Hz, being close to the expected interval of 2 to 6 Hz.

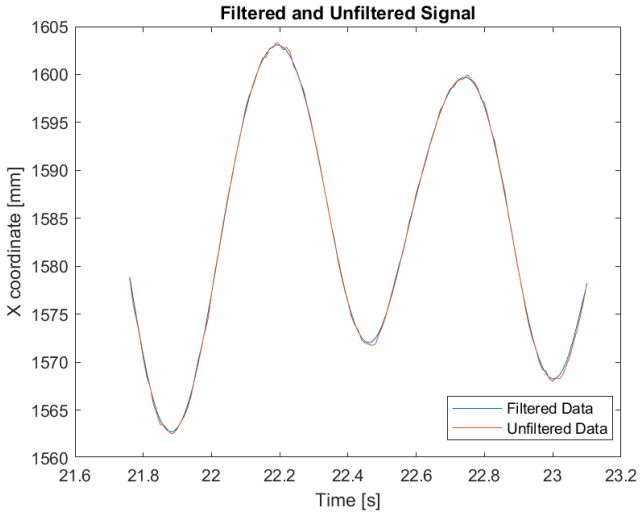

Figure B.2: Z-coordinate of the head over time, for the gait cycle. The orange line corresponds to the unprocessed raw data, whereas the blue line is the data filtered with a fourth-order zero-lag low-pass digital filter.

Note that, the faster the motion, higher cut-off frequencies are expected, since there is a faster change on the positions, being associated with higher frequencies.

Appendix C

Table C.1: Structure considered for the input file to be given to the kinematic analysis code regarding the system's initial configuration, BiomechanicalModel_gait.txt and BiomechanicalModel_mountain_climber.txt.

NBodies	**NRevolute**		**NGround**		**NDriver**			
Body number (1, ..., 14)	x_i		y_i		θ_i		PCoM	Length i
Joint Revolute number (1, …, 13)	Proximal Body, i	Distal Body, j	ξ_i	η_i	ξ_i	η_i		
Joint Driver number (1, …, 16)	Type	Proximal Body	Coordi	Distal Body	Coordj	Filename		
	I III	i i	1, 2, 3 -	- j	- -	.txt .txt		
Tstart	Tstep	Tend						